BioNanoScience (2022) 12:1158–1165
https://doi.org/10.1007/s12668-022-01019-4

Anticancer Activity of Diarachidonyl Phosphatidyl Choline Liposomal Curcumin Coated with Chitosan Against Breast and Pancreatic Cancer Cells

Riham El Kurdi[1] · Joelle Mesmar[2] · Maria Estephan[1] · Adnan Badran[3] · Elias Baydoun[2] · Digambara Patra[1]

Accepted: 26 July 2022 / Published online: 16 August 2022

Abstract
The distinctive capacity of liposomal systems to entrap both lipophilic and hydrophilic compounds allows the encapsulation of different kinds of drugs into these vesicles. Curcumin is known for its poor aqueous solubility, low bioavailability, and rapid metabolism. To inhibit these limitations, curcumin is mainly encapsulated in liposomes. Generally, DMPC, DPPC, and DSPC liposomes are widely used as a vehicle to encapsulate curcumin. Thus, in our work, curcumin was encapsulated, for the first time, into the bilayer of diarachidonyl phosphatidyl choline liposomes (DAPC), coated by a protective layer using chitosan oligosaccharides lactate (DAPC-Cur-COL NCs). Our results showed that DAPC liposomes ensured an encapsulation efficiency equal to 90% due to its long carbonyl chain compared to others liposomes. Hence, the presence of chitosan increased the encapsulation efficiency of curcumin to 99.40%. The formed nanocapsules were small in size and their anticancer potential was investigated. Interestingly, DAPC-Cur-COL NCs inhibited the proliferation of MCF-7 and Capan-1 cell lines by 85% and 90%, respectively.

Keywords Curcumin · DAPC · Cancer · MCF-7 · Capan-1

1 Introduction

Worldwide, cancer is considered the second cause of death. Based on the cancer statistics done by the World Health Organization, in 2020, 19,292,789 cases suffered from cancer where 9,958,133 deaths were recorded due to this disease [1]. The principal percentage of cancer types that occurs in men are found in the prostate, pancreas, lung and bronchus, and urinary bladder, whereas, in women, cancer prevalence is highest in the breast, pancreas, lung and bronchus, and thyroid [2]. These facts show that pancreatic and breast cancer constitute the most frequent cancer in men and women, respectively [3]. Breast cancer is a gathering of diverse malignancies that exhibits in the mammary glands [4]. Initially, nicotine stimulates breast cancer metastasis by stimulating N_2 neutrophils, creating a pre-metastatic niche in the lung [5]. Several human breast cancer cell lines have been isolated from metastatic breast cancer specimens. The most common is MCF-7, an estrogen receptor (ER)-positive cell line derived from a pleural effusion in a patient with breast cancer [6]. Pancreatic adenocarcinoma (PA) is a violent disease that grows initially in a symptom-free way and is frequently advanced at the time of diagnosis [7]. It occurs in the 70 s and rarely before the age of 40 [8]. The main causes for pancreatic cancer include tobacco smoking [9] and obesity [10]. Current treatment regimens against cancer include surgery, radiation, and chemotherapy [11]. However, these are often associated with undersirable and severe side effects or even ineffective [12]. This mandates that alternative approaches be sought to develop novel treatments with negligible effects. Accordingly, nanotechnology has been gaining more and more interest as an adequate alternative for cancer remedy [13]. Indeed, nanotechnology possesses the potential to enhance the selectivity and strength of

✉ Elias Baydoun
eliasbay@aub.edu.lb

✉ Digambara Patra
dp03@aub.edu.lb

[1] Department of Chemistry, American University of Beirut, Beirut, Lebanon

[2] Department of Biology, American University of Beirut, Beirut, Lebanon

[3] Department of Basic Sciences, University of Petra, P.O. Box 961343, Amman, Jordan

chemical, physical, and biological methodologies for stimulating cancer cell death, while diminishing collateral toxicity to nonmalignant cells. Hence, materials on the nanoscale level are been used increasingly to treat cancer cells using both active and passive targeting [14]. Liposomes are on one of the most used nanomaterials for cancer treatment. Liposomes nanocapsules consist of spheres in the range of 10–100 nm, composed either from a natural or synthetic phospholipid bilayer membrane and a water phase core [15]. In fact, the actual primary generation of nanoparticles based therapy involved lipid systems like liposomes, which are FDA approved. Henceforth, liposomes can entrap different drugs and/or inorganic nanoparticles. These properties led to an increase in their usage with an emphasis on drug delivery, imaging, and therapeutics functions [16]. Based on the amphiphilicity of phospholipids, hydrophobic drugs can be easily incorporated in the bilayer membrane [17]. Curcumin, defined as the active ingredient of the *Curcuma longa* plant, has expected great devotion over the past two decades as an antioxidant, anti-inflammatory, and anticancer agent [18]. Curcumin alone has been show to inhibit the proliferation of different cancer cell lines, including the human cervical carcinoma [19], breast cancer [20], pancreatic cancer [21], colorectal cancer [22], etc. However, this yellow compound aches from its low oral bioavailability, which obstructs its application as a therapeutic agent [23]. Accordingly, the encapsulation of curcumin into the bilayers of liposomes stabilizes the loaded curcumin proportionally to its content and increases its solubility [24]. Curcumin has been frequently encapsulated into the bilayer of DMPC, DPPC, and DSPC liposomes in order to enhance its anticancer activity [25, 26]. In this work, a new phospholipids which is diarachidonyl phosphatidyl choline (DAPC) liposomes will be used for the first time to encapsulate curcumin, and its anticancer activity against MCF-7 breast cancer cell lines and Capan-1 pancreatic cancer cell lines will be investigated.

2 Materials and Methods

2.1 Materials

DAPC (1,2-diarachidoyl-sn-glycero-3-phosphocholine) was obtained from Avanti Polar Lipids (England, CAS: 61596–53-0). The stock solution of membrane was prepared in 50 mM mono- and dibasic phosphate buffer at pH 7.0 gotten from Sigma Aldrich (Germany, CAS: 10028–24-7). Curcumin was obtained from Acros Organics (Belgium, CAS: 458–37-7). Chitosan oligosaccharide lactate (Germany, CAS: 148411–57-8), fetal bovine serum (FBS) (US, MDL: MFCD00132239), phosphate-buffered saline (PBS) (Germany, MDL: MFCD00131855), and trypsin (Germany, CAS: 9002–07-7) were obtained from Sigma Aldrich. Ethanol (Belgium, CAS: 64–17-5) and chloroform (Belgium, CAS: 67–66-3) are of spectroscopic grade and were obtained from Acros Organics. Thiazolyl blue tetrazolium bromide (MTT) (Belgium, CAS: 298–93-1) and dimethyl sulfoxide (DMSO) (Belgium, CAS: 67–68-5) were purchased from Arcos Organics. Dulbecco's Modified Eagle's medium (DMEM) (Switzerland, No: BE12-614F) and penicillin/streptomycin (Switzerland, No: 09-757F) were obtained from Lonza.

2.2 Preparation of Liposomal Curcumin Nanocapsule With/Without Chitosan

DAPC liposomal curcumin (DAPC-Cur NCs) were prepared based on the thin-film method. First, 10 mg of DAPC powder were dissolved in 2.5 mL of ethanol and 2.5 mL of chloroform, and then sonicated for 2 min to ensure a complete dissociation of the phosphocoline powder. In a second step, 1.84 mg of curcumin were dissolved in 0.5 mL of ethanol before adding 0.5 mL of chloroform to the mixture. In a next step, the mixture was evaporated using a rotary evaporator at 35–40 °C in order to evaporate the organic solvent and facilitate the formation of the thin film. Afterward, the acquired thin film was dried under oven vacuum at 45 °C for 5 h to ensure the full evaporation of the organic solvents used. Later on, the film was dissolved in 5 mL of phosphate buffer at pH = 7. The mixture was then heated for 30 s and vigorously vortexed for another 30 s at 85 °C, which is 10 °C above the phase transition temperature. This step was done for 10 min to guarantee the total dissolution of the thin film.

As for the liposomal curcumin coated with chitosan (DAPC-Cur-COL NCs), 1 mg of chitosan oligosaccharide lactate was dissolved in 1 mL of buffer at pH = 7 and added to the mixture.

Finally, for both nanocapasules, the solution was centrifuged at 15,000 rpm and the precipitate was dissolved in 5 mL of buffer at pH = 7. The solution was sonicated for 10 min before each analysis to prevent the nanocapsules aggregation.

2.3 Characterization Technique

The zeta potential was measured using the dynamic light scattering machine (Manufacturer: Particulate systems, Model: NanoPlus HD Zeta Potential/Nano Particle analyzer). The absorption spectra were recorded at room temperature using a JASCO V-570 UV–VIS-NIR spectrophotometer in the wavelength range of 200–800 nm in a 3 mL cuvette. Fluorescence spectrum and synchronous fluorescence were measured using a Jobin–Yvon-Horiba Fluorolog III fluorometer and the FluorEssence program. The excitation source was a 100-W Xenon lamp and the detector used was the R-928 instrument operating at a voltage of 950 V

with excitation and emission slits width at 5 nm. The X-ray diffraction (XRD) data were collected using a Bruker d8 discover X-ray diffractometer equipped with Cu-Ka radiation ($\lambda = 1.5405$ Å). The monochromator used was a Johansson type monochromator.

2.4 Encapsulation Efficiency and Drug Loading

After centrifugation, the supernatant was collected and its absorbance was measured using UV–Vis spectrophotometry at $\lambda = 428$ nm. The mass of the free curcumin was calculated based on the absorbance of the supernatant using Beer-Lambert's law as below:

$$A = \frac{m}{M \times V} \times \varepsilon \times l$$

where A is the absorbance of the supernatant, m is the mass of free curcumin in g, V is the volume of the supernatant in mL, M is the molar mass in g mol^{-1}, ε is the molar extinction coefficient of curcumin in M^{-1} cm^{-1}, and l is the optical path length in cm.

As for drug loading, the precipitate was freeze-dried for 24 h and the mass of the dried nanocapsules was measured. The formulas used to calculate the encapsulation efficiency (EE) and drug loading (LC) are given below [27]:

$$LC = \frac{mass\ of\ curcuminen\ capsulated\ in\ liposomes}{mass\ of\ dried\ nanocapsules} \times 100$$

$$EE = 1 - \frac{A \times \varepsilon \times V}{n0} \times 100$$

where V is the volume of the solution in mL and n_0 is the initial number of mole of curcumin in moles. The molar extinction coefficient was calculated based on the calibration curve of curcumin at pH 7.

2.5 Culture of MCF-7 and Capan-1 Cancer Cells

MCF-7 and Capan-1 cells were cultured in a complete DMEM high glucose media, supplemented with 10% FBS and 1% penicillin/streptomycin; MCF-7 and Capan-1 cells were cultured in 10-mm petri dishes and kept at 37 °C in an incubator with a humidified atmosphere containing 95% O_2 and 5% CO_2.

2.6 Cell Vialibity Assay

Cell viability was carried out using the 3-(4,5-dimethylthiazol-2-yl)-2,5-diphenyltetrazolium bromide (MTT) reduction assay. For this, cells were seeded at a density of 5000 cells per well in 96-well plates and allowed to grow until they reached 30–40% confluency. The cells were treated consequently with curcumin, chitosan, DAPC, DAPC-Cur NCs, and DAPC-Cur-COL NCs, with a concentration equal to 22 µM. The analysis was evaluated for 3 different days in order to assess the pathway of the different treatment. For this reason, the cells were incubated for 24, 48, and 72 h. Cell growth was determined as the proportional vialibility of the treated cells compared to the untreated control ones, which were assumed to have 100% viability. The assays were performed in triplicates and repeated three times. Results are presented as mean values ± SEM.

3 Results and Discussion

3.1 Characterization of DAPC-Cur-COL NCs

The preparation of liposomal curcumin was carried out based on the thin-film hydration method [28, 29]. This method is considered one of the simplest ways to prepare liposomes and involves the formation of a thin lipid film in a vial after the evaporation of the organic solvents. Afterwards, the addition of a dispersion medium gives heterogeneous liposomes [30]. One important limitation of liposomes is their short half-life and the leakage of the encapsulated drug [31]. For this reason, a chitosan oligosaccharide was added as a coating layer on the surface on the liposomal curcumin. The UV–visible and the fluorescence emission spectra of free curcumin and the prepared nanocapsules are depicted in Fig. 1A and B, respectively. Curcumin's spectra were recorded by dissolving curcumin in methanol. Generally, curcumin dissolved in methanol shows a broad characteristic UV–visible absorption peak at around 350–500 nm with an absorption peak at $\lambda = 425$ nm (see Fig. 1A) [32]. This absorption wavelength was red shifted to reach a maximum at $\lambda = 462$ nm for DAPC-Cur-COL. This shift is due to the deprotonation of curcumin induced by the strong bonding with chitosan molecule, forcing thereby the penetration of curcumin into the hydrophobic pocket of DAPC liposomes, reducing therefore the quantity of free curcumin present in the solution. This bonding is also confirmed when measuring the fluorescence emission spectrum where the emission wavelength was blue shifted from 555 to 516 nm (see Fig. 1B). In fact, this shift shows that curcumin is strongly portioning into the vesicle of DAPC liposomes. This is initially due to the transfer of curcumin from polar to less polar environment. Henceforth, similar results were obtained with El Khoury et al. [33] when encapsulating curcumin into DMPC liposomes [27].

Resonance Rayleigh Scattering (RRS) spectrum was measured by applying synchronous fluorescence spectroscopy (SFS) and keeping the wavelength interval ($\Delta\lambda$) at 0 nm (see Fig. 1C) [34]. Synchronous flurescence spectrum for free curcumin exhibited two significant peakes at ~ 380 nm and ~ 501 nm. SFS spectra showed an additional two peaks in the formed nanocapsules approximately

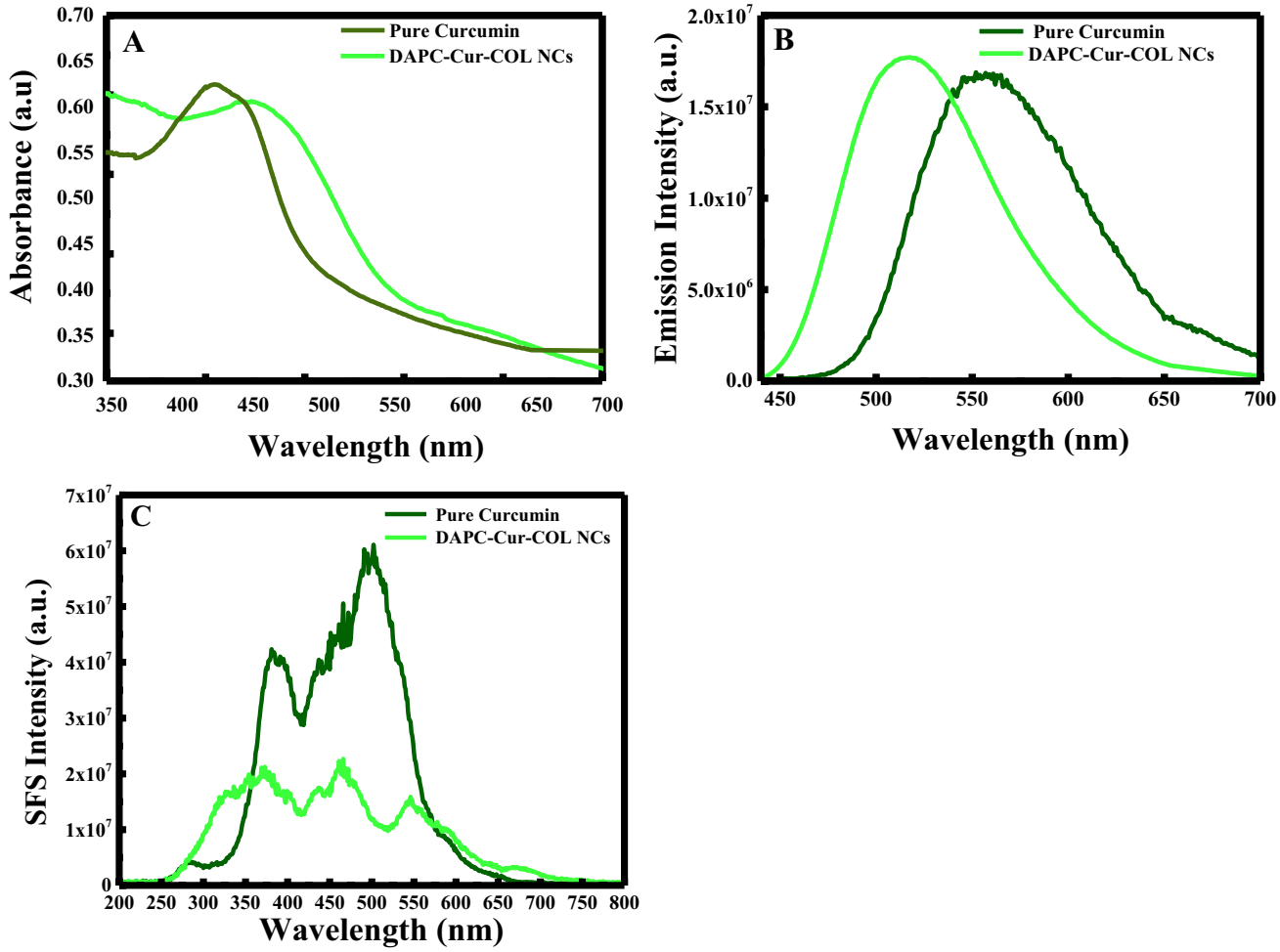

Fig. 1 **A** Uv–Visible spectrum of pure curcumin and DAPC-Cur-COL nanocapsules; **B** fluorescence emission spectrum of pure curcumin and DAPC-Cur-COL nanocapsules; and **C** SFS spectrum of pure curcumin and DAPC-Cur-COL nanocapsules

at ~ 325 nm and ~ 548 nm. In comparison with the SFS peaks of curcumin, a blue shift at ~ 325 nm and ~ 475 nm appeared for the DAPC-Cur-COL NCs. Thereby, the appearance of new peaks and the presence of a blue shift assure the effect of COL layer surrounding the liposomal curcumin surface where the encapsulation of curcumin in the bilayer of the liposomes is enhanced.

Moreover, X-ray diffraction analysis was established and the results depicted in Fig. 2. As is clearly observed, curcumin diffraction peak were observed in the range of the 2θ from 10°–30° [34]. These diffraction peaks reveal the high crystallinity nature of curcumin. Hence, DAPC-Cur-COL NCs have shown a complete amorphous structure, where all the diffraction peaks were totally absent. In fact, the crystallinity degree of pure curcumin was equal to 78.8%, where the nanocapsules showed a crystallinity degree equal to 9.5%. The decrease in the crystallinity degree proves the amorphous structure of the prepared NCs and, therefore,

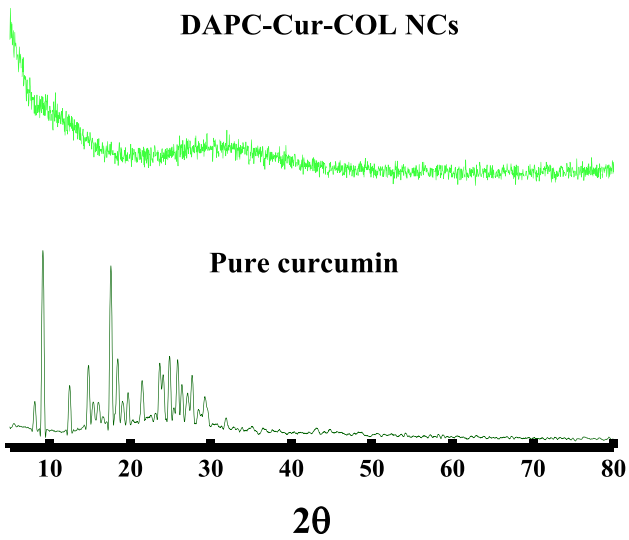

Fig. 2 X-ray diffractogram of pure curcumin and DAPC-Cur-COL nanocapsules

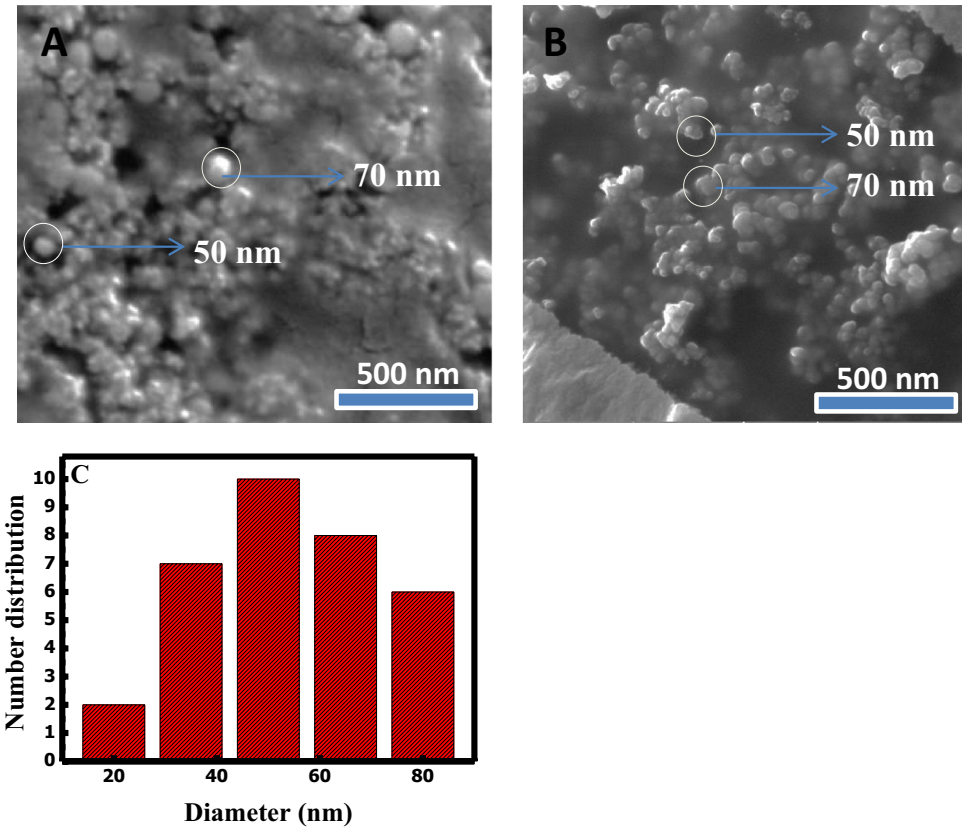

Fig. 3 SEM image of DAPC liposomal curcumin **A** in the presence of chitosan; **B** in the absence of chitosan; and **C** the dynamic light scattering analysis of the formed NCs

demonstrates the total entrapment of curcumin into the liposomal bilayers.

The use of nanocapsules as anticancer agent requires two essential parameters: their size and surface charge. Whenever the nanocapsules are smaller in size and possess a positive surface charge, their potential in inhibiting the proliferation of cancerous cell increases [35]. It is obvious from Fig. 3A that the prepared DAPC-Cur-COL NCs showed a very small size ranging between 30 and 70 nm. Hence, the addition of chitosan did not alter the size of the produced NCs were the SEM analysis for DAPC-Cur NCs in the absence of chitosan have shown the presence of spherical NCs in the size range of 50–70 nm (see Fig. 3B). Henceforth, the DLS analysis has proven the small size of the formed NCs were the analysis shows a size range between 20 and 80 nm ± 3 nm. In addition, their zeta potential value was equal to + 5.95 mV, related to the presence of chitosan owing an amino group. Hence, a study done by Smith et al. had proven that the liposomes maintain their stability for a zeta potential value between − 45 mV and + 25 mV [36]. The difference in the zeta value is generally due to the surface modifications, pH, temperature, etc.

3.2 Encapsulation Efficiency and Drug Loading

Polymers are usually used as a protective layer for the drug and the nanocapsule. In this context, chitosan was used in order to enhance the encapsulation of curcumin into the liposomal membrane, with the aim to inhibit the release of the drug. The role of chitosan was verified by calculating the value of the encapsulation efficiency and loading capacity in the absence and presence of chitosan.

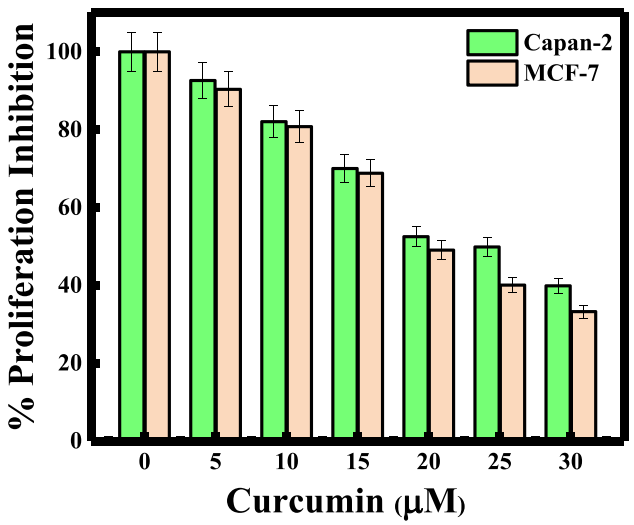

Fig. 4 Curcumin cytotoxicity effect against MCF-7 and Capan-1 cell lines

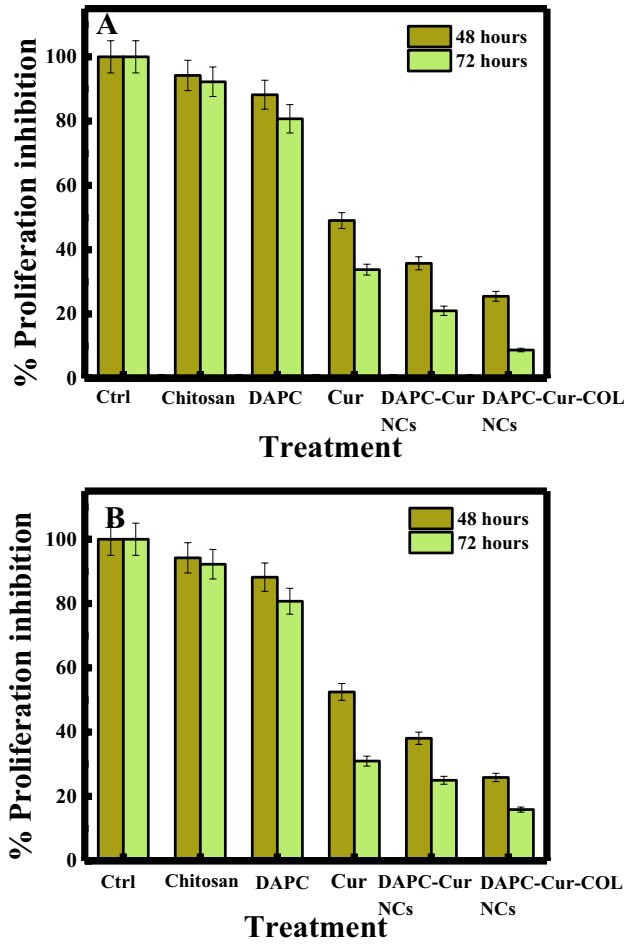

Fig. 5 Cytotoxicity effect of different treatment against **A** Capan-1 and **B** MCF-7 cancerous cell lines respectively

The concentration of free curcumin in the supernatant was calculated using the Beer-Lambert law. The EE and LC percentages were calculated based on the equations mentioned in Section II.4 and summarized in Table 2.

The drug loading content was found to be equal to 17.17% and 26.71% for the nanocapsules prepared without and with chitosan, respectively. The encapsulation efficiency of the nanocapsule prepared without chitosan was equal to 91%. The high encapsulation efficiency and drug loading percentages obtained were due to the long chain of DAPC. Similar results were obtained by Li et al. where they have proven the effect of carbonyl chain on the increase of the LC and EE percentage [37]. Also, the encapsulation efficiency of curcumin in DAPC was enhanced in the presence of chitosan, where it was found to be equal to 99.40%. This is expected as the drug loading percentage must increase with the addition of a polymer layer. This is in a good agreement with previous findings where it was clearly demonstrated that the drug loading and encapsulation efficiency of curcumin increased in the presence of a coating layer. However, the role of chitosan as a protective layer was also confirmed by Hasan et al. where the encapsulation efficiency of liposomal curcumin increases from 65% in the absence of chitosan to 88% in the presence of chitosan [38].

3.3 Anticancer Cctivity of DAPC-Cur-COL NCs Against MCF-7 and Capan-1 Cancerous Cells

a) Cytotoxicity effect of curcumin against MCF-7 and Capan-1 cell lines

Curcumin has been described as an anticancer agent by inhibiting the proliferation of cancerous cells through the induction apoptosis and by reducing the invasiveness of cancers cells through various cellular signaling pathways [18].

In this study, MCF-7 and Capan-1 cancer cell lines were exposed to different concentrations of curcumin in the range of 0–30 µM for 48 h. The half maximal inhibitory concentration (IC_{50}) was measured. As shown in Fig. 4, the IC_{50} of curcumin was established to be equal to ~ 22 µM and ~ 20 µM for MCF-7 and Capan-1, respectively. These values were in agreement with IC_{50} values established previously. In fact, 48 h after treatment, Mirakabad et al. have estimated the IC_{50} of curcumin to be equal to 21.32 µM for MCF-7 [39], and Sutaria et al. have established the IC_{50} of curcumin to be equal to 19.6 µM for Capan-1 cells lines [40].

b) Cytotoxicity effect of DAPC-Cur-COL against MCF-7 and Capan-1 cell lines

The activity of curcumin as an anticancer reagent is expected to be enhanced when encapsulated into liposomes, as the use of liposomes increases the activity of curcumin

Table 1 Different anticancer reagent used for Capan-1 and MCF-7 treatment

Cell type	Anticancer agent	Concentration	% proliferation	Reference
MCF-7	Gold nanoparticles	20 µg/mL	50%	[41]
	DSPC-Cur	10 µg/mL	65%	[42]
	DAPC-Cur-COL NCs	2 µg/mL	85%	Our work
Capan-1	GA-MNP-Fe_3O_4 NPs	20 µg/mL	60%	[43]
	DPPC-Cur	10 µg/mL	75%	[44]
	DAPC-Cur-COL NCs	2 µg/mL	90%	Our work

Table 2 EE and LC % for DAPC-Cur and DAPC-Cur-COL NCs

Nanocapsules	Encapsulation efficiency (%)	Drug loading (%)
DAPC-Cur NCs	91	17.17
DAPC-Cur-COL NCs	99.4	26.71

by releasing it to the specific target. The prepared liposomal curcumin coated with chitosan was tested on breast and pancreatic cancer cell lines. Based on the IC_{50} of curcumin obtained above (20 µM (3 µg/mL)), MCF-7 and Capan-1 cancer cells were treated with the same curcumin concentration using encapsulated in DAPC-Cur NCs, DAPC-Cur-COL NCs, and using DAPC and chitosan as a control. The treatment was done for 48 and 72 h. As presented in Fig. 5A and B, no remarkable effect was observed in MCF-7 and Capan-1 cells treated with chitosan and DAPC liposomes. The use of DAPC-Cur NCs and DAPC-Cur-COL NCs improved strongly the anti-proliferative potential of curcumin in Capan-1 cancer cells (Fig. 5A). For example, when treated with 20 µM (3 µg/mL), both nanocapsules showed an increase in the inhibition of proliferation by up to 65% after 48 h. And, a remarkable inhibition of proliferation was observed after 72 h in the DAPC-Cur NCs treated cells, where ~ 75% inhibition was acquired. This means that DAPC liposome improved the anticancer activity of curcumin by enhancing its target specificity. And after the same treatment duration using DAPC-Cur-COL NCs, ~ 90% inhibition of proliferation was observed. This difference in the value is linked to the presence of chitosan, which acts as a protective layer and ensures the total entrapment of curcumin into the DAPC liposomes and preventing its leakage. Similarly, DAPC-Cur-COL NCs exhibited a strong anticancer potential against MCF-7 cells, with more than 70% and 85% inhibition observed after 48 h and 72 h, respectively (see Fig. 5B).

The efficiency of our nanoparticles was compared to different anticancer reagents described in the literature and presented in Tables 1 and 2.

4 Conclusion

To sum up, the activity of DAPC-Cur-COL NCs as an anticancer agent was verified for the first time, as curcumin inhibited the proliferation of MCF-7 and Capan-1 cancer cell lines with IC_{50} values of curcumin equal to 22 and 19 µM for MCF-7 and Capan-1, respectively. And for the same concentration, the matrix liposomal curcumin coated with chitosan enhanced the anticancer activity of curcumin with percentage inhibition equal to 85% and 90% for MCF-7 and Capan-1 cell lines, respectively.

Funding Financial support was provided by the American University of Beirut, Lebanon through University Research Board (URB) grant and University of Petra, Jordan to carry out this work is acknowledged.

Declarations

Research Involving Humans and Animals Statement Not applicable.

Informed Consent Not applicable.

Consent for Publication Not applicable.

Conflict of Interest The authors declare no competing interests.

References

1. Globocan. (2020). "The global cancer observatory - all cancers,".
2. Hassanpour, S. H., & Dehghani, M. (2017). Review of cancer from perspective of molecular. *Journal of Cancer Research and Practice, 4*(4), 127–129.
3. Siegel, R. L., Miller, K. D., & Jemal, A. (2016). Cancer statistics, 2016. *CA: A Cancer Journal for Clinicians, 66*(1), 7–30.
4. Feng, Y., et al. (2018). Breast cancer development and progression: Risk factors, cancer stem cells, signaling pathways, genomics, and molecular pathogenesis. *Genes & Diseases, 5*(2), 77–106.
5. Tyagi, A., et al. (2021). Nicotine promotes breast cancer metastasis by stimulating N2 neutrophils and generating pre-metastatic niche in lung. *Nature Communications, 12*(1), 1–18.
6. Macdonald, S., Oncology, R., & General, M. (2016). Breast cancer breast cancer. *Journal of the Royal Society of Medicine, 70*(8), 515–517.
7. Deer, E. L., et al. (2010). Phenotype and genotype of pancreatic cancer cell lines. *NIH Public Access, 39*(4), 425–435.
8. Ryan, D. P., Hong, T. S., & Bardeesy, N. (2014). Pancreatic adenocarcinoma. *New England Journal of Medicine, 371*(11), 1039–1049.
9. Underwood, P. W., et al. (2020). Nicotine induces IL-8 secretion from pancreatic cancer stroma and worsens cancer-induced cachexia. *Cancers (Basel), 12*(2), 1–12.
10. Xu, M., Jung, X., Hines, J., Eibl, G., & Chen, Y. (2012). Obesity and pancreatic cancer: Overview of epidemiology and potential prevention by weight loss. *HHS Public Access, 47*(2), 93–109.
11. Newhauser, W. D., De Gonzalez, A. B., Schulte, R., & Lee, C. (2016). A review of radiotherapy-induced late effects research after advanced technology treatments. *Frontiers in Oncology, 6*, 1–11.
12. Ramirez, L. Y., Huestis, S. E., Yap, T. Y., Zyzanski, S., Drotar, D., & Kodish, E. (2009). Potential chemotherapy side effects: What do oncologists tell parents? *NIH Public Access, 52*(4), 497–502.
13. Heath, J. R., & Davis, M. (2008). Nanotechnology and cancer James. *NIH Public Access, 23*(1), 1–7.
14. Gmeiner, W. H., & Ghosh, S. (2014). Nanotechnology for cancer treatment. *Nanotechnology Reviews, 3*(2), 111–122.
15. Malam, Y., Loizidou, M., & Seifalian, A. M. (2009). Liposomes and nanoparticles: Nanosized vehicles for drug delivery in cancer. *Trends in Pharmacological Sciences, 30*(11), 592–599.
16. Patra, J. K., et al. (2018). Nano based drug delivery systems: Recent developments and future prospects 10 Technology 1007 Nanotechnology 03 Chemical Sciences 0306 Physical Chemistry (incl. Structural) 03 Chemical Sciences 0303 Macromolecular and Materials Chemistry 11 Medical and Health Sciences 1115 Pharmacology and Pharmaceutical Sciences 09 Engineering 0903

Biomedical Engineering Prof Ueli Aebi, Prof Peter Gehr. *J Nanobiotechnology, 16*(1), 1–33.
17. Bozzuto, G., & Molinari, A. (2015). Liposomes as nanomedical devices. *International Journal of Nanomedicine, 10*, 975–999.
18. Tomeh, M. A., Hadianamrei, R., & Zhao, X. (2019). A review of curcumin and its derivatives as anticancer agents. *International Journal of Molecular Sciences, 20*(5), 1–26.
19. Zhao, J., & Zhao, Y. (2004). Effects of curcumin on proliferation and apoptosis of human cervical carcinoma HeLa cells in vitro. *Chinese Journal of Cancer Research, 16*(3), 225–228.
20. Liu, J. L., et al. (2017). Curcumin inhibits MCF-7 cells by modulating the NF-κB signaling pathway. *Oncology Letters, 14*(5), 5581–5584.
21. Bimonte, S., et al. (2016). Curcumin anticancer studies in pancreatic cancer. *Nutrients, 8*(7), 1–12.
22. Pricci, M., Girardi, B., Giorgio, F., Losurdo, G., Ierardi, E., & Di Leo, A. (2020). Curcumin and colorectal cancer: From basic to clinical evidences. *International Journal of Molecular Sciences, 21*(7), 1–13.
23. Liu, W., et al. (2016). Oral bioavailability of curcumin: Problems and advancements. *Journal of Drug Targeting, 24*(8), 694–702.
24. Karewicz, A., Bielska, D., Gzyl-Malcher, B., Kepczynski, M., Lach, R., & Nowakowska, M. (2011). Interaction of curcumin with lipid monolayers and liposomal bilayers. *Colloids Surfaces B Biointerfaces, 88*(1), 231–239.
25. Thangapazham, R. L., Puri, A., Tele, S., Blumenthal, R., & Maheshwari, R. K. (2008). Evaluation of a nanotechnology-based carrier for delivery of curcumin in prostate cancer cells. *International Journal of Oncology, 32*(5), 1119–1123.
26. Feng, T., Wei, Y., Lee, R. J., & Zhao, L. (2017). Liposomal curcumin and its application in cancer. *International Journal of Nanomedicine, 12*, 6027–6044.
27. Palanikumar, L., et al. (2018). Importance of encapsulation stability of nanocarriers with high drug loading capacity for increasing in vivo therapeutic efficacy. *Biomacromolecules, 19*(7), 3030–3039.
28. Moussa, Z., Chebl, M., & Patra, D. (2017). Interaction of curcumin with 1,2-dioctadecanoyl-sn-glycero-3-phosphocholine liposomes: Intercalation of rhamnolipids enhances membrane fluidity, permeability and stability of drug molecule. *Colloids and Surfaces B: Biointerfaces, 149*, 30–37.
29. Jilani, A., Abdel-wahab, M. S., Hammad, A. H. (2017). Advance deposition techniques for thin film and coating.
30. Zhang, H. (2017). Thin-film hydration followed by extrusion method for liposome preparation. *Methods in Molecular Biology, 1522*, 17–22.
31. Daraee, H., Etemadi, A., Kouhi, M., Alimirzalu, S., & Akbarzadeh, A. (2016). Application of liposomes in medicine and drug delivery. *Artificial Cells, Nanomedicine, and Biotechnology, 44*(1), 381–391.
32. Subhan, M. A., Alam, K., Rahaman, M. S., Rahman, M. A., & Awal, R. (2013). Synthesis and characterization of metal complexes containing curcumin ($C_{21}H_{20}O_6$) and study of their antimicrobial activities and DNA-binding properties. *Journal of Scientific Research, 6*(1), 97–109.
33. El Khoury, E., & Patra, D. (2016). Length of hydrocarbon chain influences location of curcumin in liposomes: Curcumin as a molecular probe to study ethanol induced interdigitation of liposomes. *Journal of Photochemistry and Photobiology, B: Biology, 158*, 49–54.
34. El Kurdi, R., & Patra, D. (2017). The role of OH − in the formation of highly selective gold nanowires at extreme pH: Multi-fold enhancement in the rate of the catalytic reduction reaction by gold nanowires. *Physical Chemistry Chemical Physics: PCCP, 19*(7), 5077–5090.
35. Bao, H., Zhang, Q., Xu, H., & Yan, Z. (2016). Effects of nanoparticle size on antitumor activity of 10-hydroxycamptothecin-conjugated gold nanoparticles: In vitro and in vivo studies. *International Journal of Nanomedicine, 11*, 929–940.
36. Smith, M. C., Crist, R. M., Clogston, J. D., & Mcneil, S. E. (2017). Zeta potential : A case study of cationic, anionic, and neutral liposomes. *Analytical and Bioanalytical Chemistry, 45*, 1–9.
37. Li, Q., Li, X., & Zhao, C. (2020). Strategies to obtain encapsulation and controlled release of small hydrophilic molecules. *Frontiers in Bioengineering and Biotechnology, 8*(May), 1–6.
38. Hasan, M., et al. (2020). Growth-inhibitory effect of chitosan-coated liposomes encapsulating curcumin on MCF-7 breast cancer cells. *Marine Drugs, 18*(4), 1–11.
39. Mirakabad, F. S. T., et al. (2016). A Comparison between the cytotoxic effects of pure curcumin and curcumin-loaded PLGA-PEG nanoparticles on the MCF-7 human breast cancer cell line. *Artificial Cells, Nanomedicine, and Biotechnology, 44*(1), 423–430.
40. Sutaria, D., Grandhi, B. K., Thakkar, A., Wang, J., & Prabhu, S. (2012). Chemoprevention of pancreatic cancer using solid-lipid nanoparticulate delivery of a novel aspirin, curcumin and sulforaphane drug combination regimen. *International Journal of Oncology, 41*(6), 2260–2268.
41. Selim, M. E., & Hendi, A. A. (2012). Gold nanoparticles induce apoptosis in MCF-7 human breast cancer cells. *Asian Pacific Journal of Cancer Prevention, 13*(4), 1617–1620.
42. Ruttala, H. B., & Ko, Y. T. (2015). Liposomal co-delivery of curcumin and albumin/paclitaxel nanoparticle for enhanced synergistic antitumor efficacy. *Colloids and Surfaces B: Biointerfaces, 128*, 419–426.
43. Wang, C., Zhang, H., Chen, B., Yin, H., & Wang, W. (2011). Study of the enhanced anticancer efficacy of gambogic acid on Capan-1 pancreatic cancer cells when mediated via magnetic Fe3O4 nanoparticles. *International Journal of Nanomedicine, 6*, 1929–1935.
44. Ranjan, A. P., Mukerjee, A., Helson, L., Gupta, R., & Vishwanatha, J. K. (2013). Efficacy of liposomal curcumin in a human pancreatic tumor xenograft model: Inhibition of tumor growth and angiogenesis. *Anticancer Research, 33*(9), 3603–3610.